Novel small molecular dye-loaded lipid nanoparticles with efficient near-infrared-II absorption for photoacoustic imaging and photothermal therapy of hepatocellular carcinoma

Qingshan Chen[1*], Jingqin Chen[2*], Mu He[1], Yuanyuan Bai[2], Huixiang Yan[4], Ning Zeng[1], Fangyan Liu[2], Sai Wen, Liang Song[2], Zonghai Sheng[3#], Chengbo Liu[2#], Chihua Fang[1#]

Author information:

1. Department of Hepatobiliary Surgery, Zhujiang Hospital, Southern Medical University, Guangzhou, 510280, PR China.
2. Research Laboratory for Biomedical Optics and Molecular Imaging, Shenzhen Key Laboratory for Molecular Imaging, Institute of Biomedical and Health Engineering, Shenzhen Institutes of Advanced Technology, Chinese Academy of Sciences, Shenzhen 518055, China.
3. Paul C. Lauterbur Research Center for Biomedical Imaging, Institute of Biomedical and Health Engineering, Shenzhen Institutes of Advanced Technology, Chinese Academy of Sciences, Shenzhen 518055, China.
4. Department of Ultrasonography, The Eighth Affiliated Hospital, SUN YAT-SEN University, Shenzhen, 518033, China.

[#] Corresponding author. Chihua Fang, E-mail: fangch_dr@163.com

[#] Corresponding author. Chengbo Liu, E-mail: cb.liu@siat.ac.cn

[#] Corresponding author. Zonghai Sheng, E-mail: zh.sheng@siat.ac.cn

[*]These authors contributed equally to this work

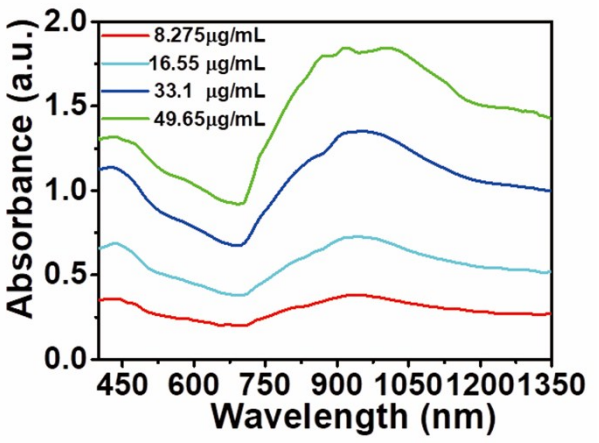

Figure S1. UV−vis absorbance of the Polipo-IR NPs with various concentrations.

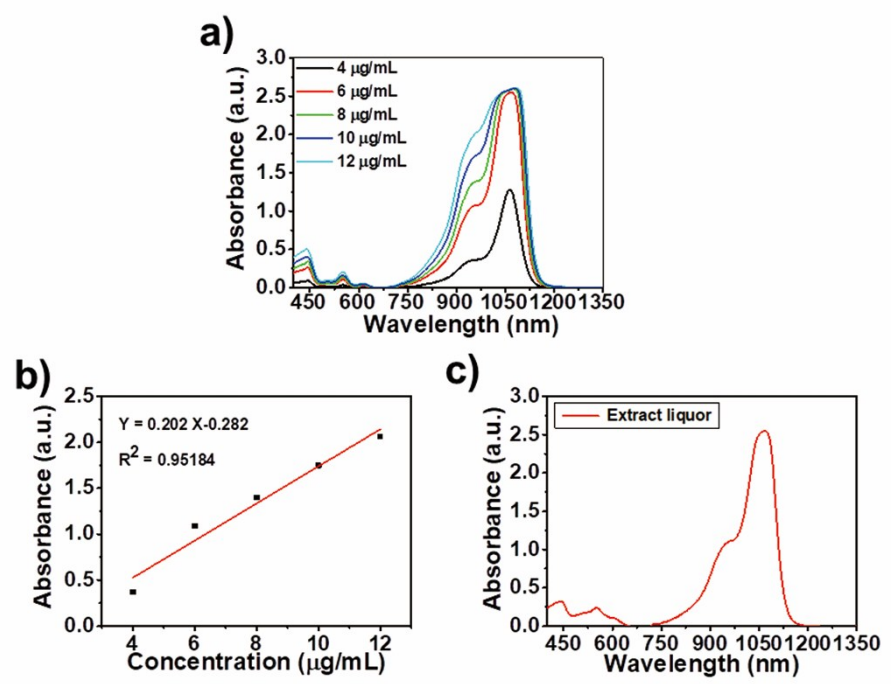

Figure S2. The loading amount of dyes in Polipo-IR NPs. **(a)** UV−vis absorbance of the IR 1061 in CCL_2 with various concentrations, **(b)** The Linear fit equation of UV-vis absorbance at 970 nm. **(c)** The UV-vis absorbance of extract liquor.

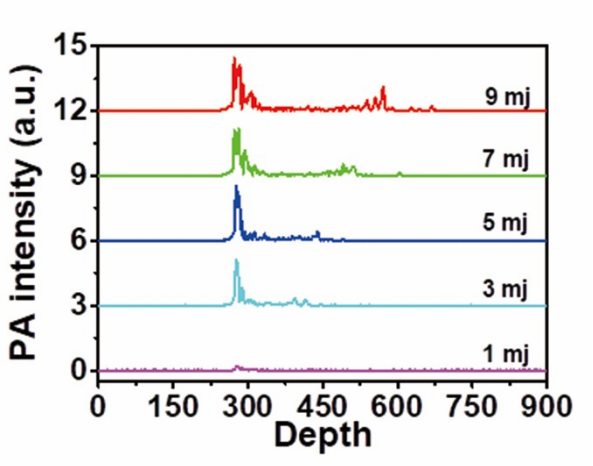

Figure S3. PA intensities of Polipo-IR NPs with different laser powers.

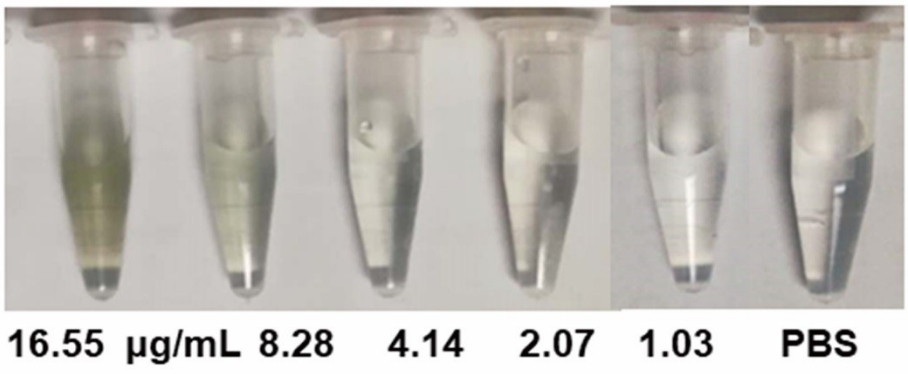

Figure S4. Photograph of various concentrations of Polipo-IR NPs at the same laser power.

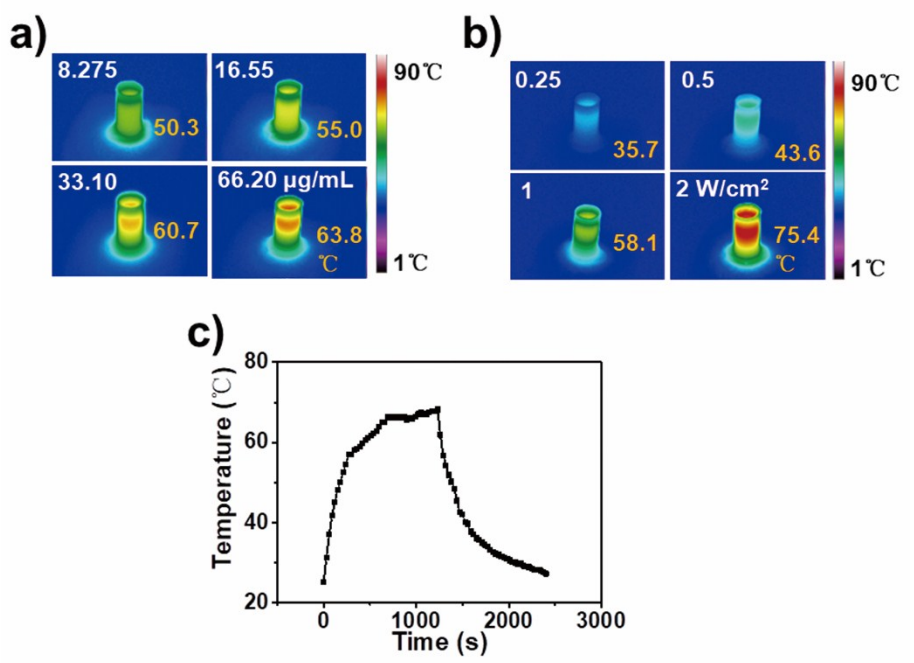

Figure S5. Photothermal property of Polipo-IR NPs. IR images of temperature changes of Polipo-IR NPs aqueous solution with various (a) concentrations under the laser irradiating powers (1064 nm, 1.0 W/cm^2) and **(b)** laser power with aqueous solution of 33.1 μg/mL. **(c)** Photothermal performance of Polipo-IR NPs dispersed in aqueous solution under 1064 nm laser irradiation (1 W/cm^2), the laser was turned off when the temperature became stable (33.1 μg/mL, 1 mL).

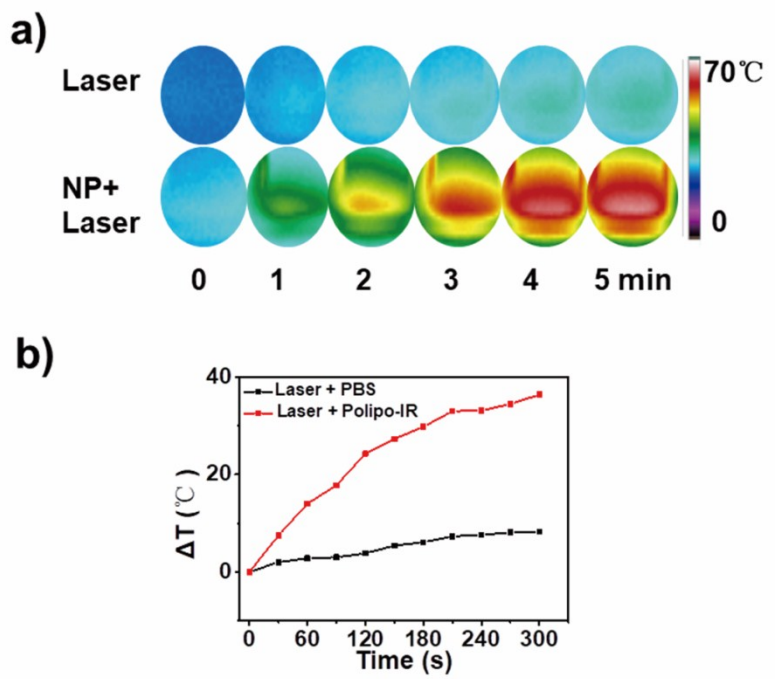

Figure S6. *In vitro* biocompatibility and PTT. **(a)** NIR thermal images of Hep-G2 cells in the laser group and Polipo-IR NPs + Laser group. **(b)** Temperature changes of *in vitro* cytotoxicity against Hep-G2 cells in two groups.

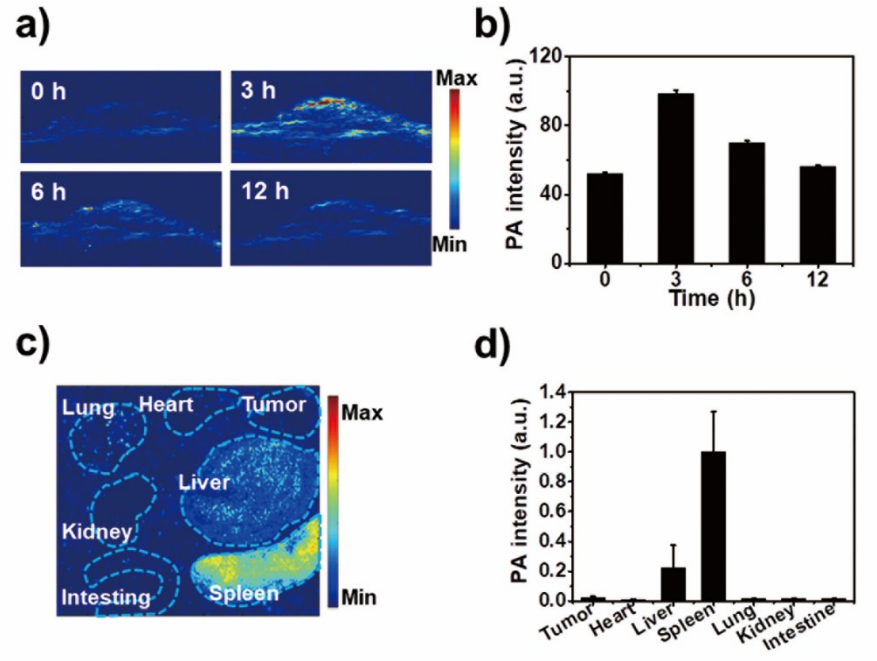

Figure S7. The clearance and biodistribution of the Polipo-IR NPs after intravenous injection. (a) The B-scan images of the Polipo-IR NPs at different time points (0, 3, 6, 12 h) after administration. **(b)** Quantitative analysis of PA signals in tumor sites. **(c)** The PA imaging of organs that demonstrated the biodistribution of the Polipo-IR NPs directly. **(d)** Quantitative analysis of PA signals in various organs.

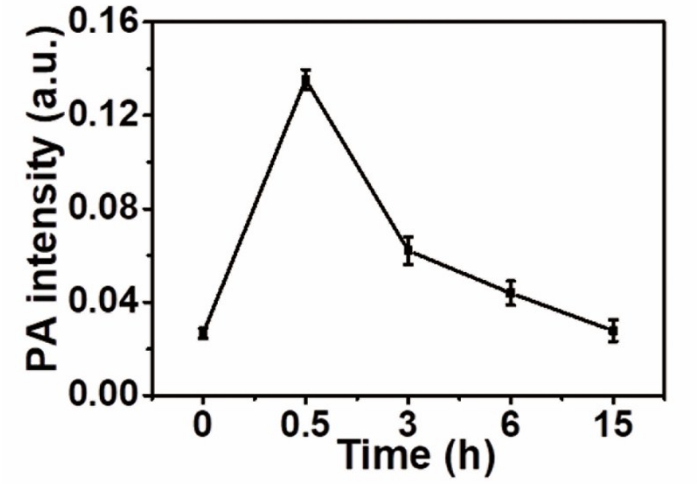

Figure S8. The blood circulation of the Polipo-IR NPs after intravenous injection.

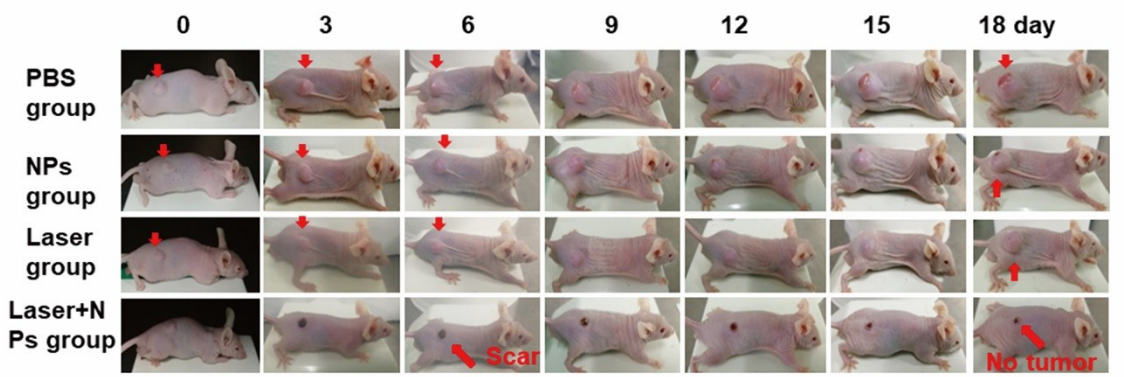

Figure S9. Representative in vivo photothermal therapy photos of mice bearing subcutaneous Hep-G_2 tumors (PBS group, Polipo-IR NPs group, laser group and Laser + Polipo-IR NPs group).

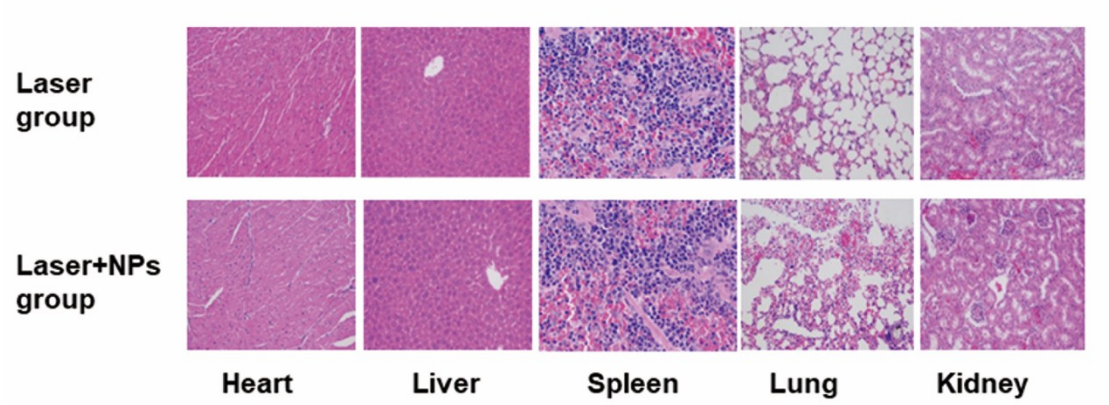

Figure S10. Representative hematoxylin and eosin (H&E) stained images of major organs (heart, liver, spleen, lung and kidney) which were collected from the mice sacrificed after 18 days of NPs injection (magnification: 200 ×)

Calculation of photothermal conversion efficiency of Polipo-IR NPs

Following the Roper's approach[1], the total energy balance for Polipo-IR NPs can be calculated using equations:

(1)

$$\eta = \frac{hS(T\text{max} - T\text{surr}) - Qis}{I(1 - 10 \text{ - A1064})}$$

(2)

$$hS = \frac{\text{mCwater}}{\tau s}$$

(3)

$$t = -\ \tau s \text{In}\theta = -\ \tau s \text{In}\ (\frac{T - T\text{surr}}{T\text{max} - T\text{surr}})$$

(4)

$$Qdis = \frac{mC\text{H2O}(T\text{max}(\text{water}) - T\text{surr})}{\tau\text{water}}$$

where h is the heat transfer coefficient, S is the surface area of the container, m is the mass of products (m = 0.9985 g), τs is a system time constant (434.31 s), C_{water} is specific heat capacity of solvent (C_{water} =4.2 J/g •°C), I is incident laser power (1.0 W/cm^2), η is the photothermal conversion efficiency, A is the absorbance of Polipo-IR NPs (A_{1064} = 1.22) , T_{surr} is the ambient temperature of the surroundings. T_{max} and $T_{max(water)}$ are the equilibrium temperature of Polipo-IR NPs solution and water, respectively. The Polipo-IR NPs photothermal conversion efficiency (η) for continuous laser of 1064 nm is calculated to be 45.25%.

Table S1: Photothermal conversion efficiency of contrasts of the nanoparticles (1064 nm)

Agents	Wavelength (nm)	Photothermal conversion	Reference

		efficiency(η)	
Polipo-IR	1064	45.25%	This study
SPNI-II [2]	1064	43.4%	*Adv Mater,* 2018, **30**, e1705980.
PEG-MoOx NPs [3]	1064	37.4%	*Nanoscale,* 2018, **10**, 1517.
Fe_3O_4@CuS [4]	1064	19.2%	*Advanced Functional Materials,* 2015, **25**, 6527.
IONP@shell-in-shell [5]	1064	28.3%.	*ACS Appl. Mater. Interfaces* 2018, **10**, 1508.
$Nb_{0.12}$-TiO_2-PEG [6]	1064	40.6%	*Nanoscale,* 2017, **9**, 9148.
$(NH4)_xWO_3$ [7]	1064	39.4%	*Biomaterials,* 2015, **52**, 407.
TiO_2−x [8]	1064	39.8%	*ACS Nano,* 2018, **12**, 4545.
2D Nb_2C MXenes [9]	1064	28.6%	*Theranostics,* 2018, **8**, 4491.
PEGylated Cu_3BiS_3 [10]	1064	40.7%,	*Biomaterials,* 2017,**112**, 164.
AuNR-Glu [11]	1064	43.12%	*J Agric Food Chem,* 2018, **66**, 4091.
Au-Cu_9S_5 [12]	1064	37%	J *Am Chem Soc,* 2014, **136**, 15684.

References

1. Du L, Qin H, Ma T, Zhang T and Xing D. *ACS Nano*, 2017, **11**,8930.

2. Jiang Y, Li J, Zhen X, Xie C and Pu K. *Adv Mater,* 2018, **30**, e1705980.

3.Yin W 1, Bao T, Zhang X, Gao Q, Yu J, Dong X, Yan L, Gu Z and Zhao Y. *Nanoscale* 2018, **10**, 1517.

4. Ze-Cong Wu, Wei-Peng Li, Cheng-Hung Luo, Chia-Hao Su and Chen-Sheng Yeh. *Advanced Functional Materials,* 2015, **25**, 6527.

5. Ming-Fong Tsai, Chin Hsu, Chen-Sheng Yeh, Yu-Jen Hsiao, Chia-Hao Su and Li-Fang Wang. *ACS Appl. Mater. Interfaces,* 2018, **10**, 1508.

6. Yu N, Hu Y, Wang X, Liu G, Wang Z, Liu Z, Tian Q, Zhu M, Shi X and Chen Z. *Nanoscale,* 2017, **9**, 9148.

7. Guo C, Yu H, Feng B, Gao W, Yan M, Zhang Z, Li Y and Liu S. *Biomaterials,* 2015, **52**, 407.

8. Han X, Huang J, Jing X, Yang D, Lin H, Wang Z, Li P and Chen Y. *ACS Nano,* 2018, **12**, 4545.

9. Han X, Jing X, Yang D, Lin H, Wang Z, Ran H, Li P and Chen Y. *Theranostics,* 2018, **8**, 4491.

10. Li A, Li X, Yu X, Li W, Zhao R, An X, Cui D, Chen X and Li W. *Biomaterials* 2017,**112**, 164.

11. Li X, Zhou J, Dong X, Cheng WY, Duan H and Cheung PCK. *J Agric Food Chem* 2018, **66**,4091.

12. Ding X, Liow CH, Zhang M, Huang R, Li C, Shen H, Liu M, Zou Y, Gao N, Zhang Z, Li Y, Wang Q, Li S and Jiang J. J *Am Chem Soc,* 2014, **136**,15684.